Heat capacity, Raman, and Brillouin scattering studies of $M_2O-MgO-WO_3-P_2O_5$ glasses (M=K,Rb)

M. Maczka, J. Hanuza, and J. Baran
Institute of Low Temperature and Structure Research, Polish Academy of Sciences, P.O. Box 1410, 50-950 Wroclaw 2, Poland

A. Hushur and S. Kojima
Institute of Materials Science, University of Tsukuba, Ibaraki 305-8573, Japan

(Received 21 July 2006; accepted 7 November 2006; published online 26 December 2006)

The authors report the results of temperature-dependent Brillouin scattering from both transverse and longitudinal acoustic waves, heat capacity studies as well as room temperature Raman scattering studies on $M_2O-MgO-WO_3-P_2O_5$ glasses (M=K,Rb). These results were used to obtain information about structure and various properties of the studied glasses such as fragility, elastic moduli, ratio of photoelastic constants, and elastic anharmonicity. They have found that both glasses have similar properties but replacement of K^+ ions by Rb^+ ions in the glass network leads to decrease of elastic parameters and P_{44} photoelastic constant due to increase of fragility. Based on Brillouin spectroscopy they show that a linear correlation between longitudinal and shear elastic moduli holds over a large temperature range. This result supports the literature data that the Cauchy-type relation represents a general rule for amorphous solids. An analysis of the Boson peak revealed that the form of the frequency distribution of the excess density of states is in agreement with the Euclidean random matrix theory. The reason of the observed shift of the maximum frequency of the Boson peak when K^+ ions are substituted for Rb^+ ions is also briefly discussed.
 [DOI: 10.1063/1.2403127]

I. INTRODUCTION

An adequate understanding of many features accompanying glass formation as well as the glassy state itself is of considerable interest. These features have been studied with help of many experimental techniques. One of a very powerful tool in studies of glasses is Brillouin spectroscopy since it has been shown to give valuable information on the dynamical properties of glass-forming materials in the gigahertz region.[1–8] The relaxational processes have been extensively studied for glass formers without directional bonds, which show a similar high increase of viscosity upon supercooling and are called fragile systems.[3,6,7] The dynamics of these fragile systems is relatively well understood on the basis of mode coupling theory.[6,9] On the other hand, in the presence of directional bonds the temperature variation of viscosity is weaker, and the dynamics of these so-called strong and intermediate glass formers is still not well understood.[8,10] It is, therefore, of great interest to study strong and intermediate glass formers in a broad temperature range in order to understand how the presence of directional bonds influences the various properties of glasses. It is also worth to note that most of the Brillouin scattering studies deal with the behavior of the quasielastic peak and longitudinal acoustic (LA) peak whereas relatively little attention has been given to studies of transverse acoustic (TA) waves. Studies of both LA and TA modes are, however, of great interests since they provide important data on structural changes that occur in glasses, temperature dependence of viscosity, and the elastic properties of materials.[3,7,8,11]

Two other powerful techniques, frequently employed in the studies of glass-forming materials, are Raman spectroscopy and heat capacity measurements. The first technique gives information about short-range structure of glasses and allows studying the so-called "Boson peak."[12–16] Study of the Boson peak is of great interest since its origin still remains unclear.[13–16] On the other hand, heat capacity studies may provide, among others, some information on fragility, structural relaxation, and aging effects in glasses.[17–20] A particularly suitable technique for studies of glass transitions is modulated differential scanning calorimetry (MDSC) since it gives information on both real and imaginary parts of heat capacity.[17,21]

In this paper two phosphate glasses of the composition corresponding to crystalline $K_2MgWO_2(PO_4)_2$ and $Rb_2MgWO_2(PO_4)_2$ have been studied since these phosphates exhibit interesting properties. In particular, $K_2MgWO_2(PO_4)_2$ has a structure related to famous nonlinear material $KTiOPO_4$ (KTP) and exhibits optical nonlinear and ferroelectric properties.[22] These glasses provide also good opportunity to check influence of the structure on some glass properties.

II. EXPERIMENT

Glasses corresponding to $K_2MgWO_2(PO_4)_2$ (KMWPO) and $Rb_2MgWO_2(PO_4)_2$ (RbMWPO) compositions were prepared using analytical grades of M_2CO_3 (M=K,Rb), MgO, WO_3, and P_2O_5. Appropriate amounts of the starting materials were thoroughly mixed and transferred to platinum crucibles. The mixture of reagents was heated to 1133 K, kept at

this temperature for 20 h, and then cooled at a rate 100 K/h (about 0.028 K/s) to room temperature. The obtained glasses were transparent, of good optical quality, without inclusions. Glass samples were cut into 2 mm thick parallelepipeds, with their two faces optically polished.

The chemical compositions of the obtained glass samples were analyzed with help of x-ray dispersion measurements using EDAX 9800 microanalyzer. As a standard $K_2MgWO_2(PO_4)_2$ and $Rb_2MgWO_2(PO_4)_2$ single crystals have been used. The established compositions of these samples $(0.89K_2O-1.05MgO-1.04WO_3-1.12P_2O_5, 0.91Rb_2O-0.97MgO-0.98WO_3-1.11P_2O_5)$ are in good agreement with the nominal composition within experimental error.

The density of the glasses was determined by standard Archimedes technique using distilled water as the working fluid. The accuracy of the measurements was about ± 0.01 g/cm^3.

The amorphous character of the glasses was confirmed by x-ray powder diffraction analysis.

Heat capacity was measured using a Thermal Analyst 2000 calorimeter (TA Instruments). The samples were of the order of 15 mg mass. The measurements were made for a modulation frequency of 10 mHz and peak to peak temperature modulation amplitude of 1 K. The sample was heated at 2 K/min from 473 to 873 K and then cooled down to 473 K.

The Brillouin scattering spectra were obtained with a 3+3 pass tandem Sandercock-type Fabry-Pérot interferometer. A conventional photon-counting system and a multichannel analyzer were used to detect and average the signal. Both backscattering and right-angle symmetric scattering geometries of the experiments were employed for room temperature measurements. For high-temperature measurements, each sample was placed in a home-made furnace and the scattered light from the samples was collected in symmetric 90° scattering geometry. The free spectral ranges were 30 and 40 GHz for 90° and 180° scattering geometries, respectively.

Raman spectra above 100 cm^{-1} were measured in backscattering geometry with a Bruker FT-Raman RFS 100/S spectrometer and the 1064 nm excitation. Low-frequency spectra, below 200 cm^{-1}, were obtained with a triple-grating spectrometer of additive dispersion (Jobin Yvon, T64000) and 532 nm excitation. All spectra were recorded with a spectral resolution of 2 cm^{-1}.

III. RESULTS AND DISCUSSION

A. Heat capacity

Heat capacity can be described as having two components, a real component (C_p') and an imaginary component (C_p'').[17,18,23,24] The real component is the true heat capacity of the material, which is related to slow molecular motion. The imaginary component of heat capacity has been attributed to kinetic events within the sample or to dissipation processes relating to entropy production.[23,24] MDSC technique gives information on both real and imaginary parts of C_p and it is therefore a very suitable technique for studies of glass transitions.

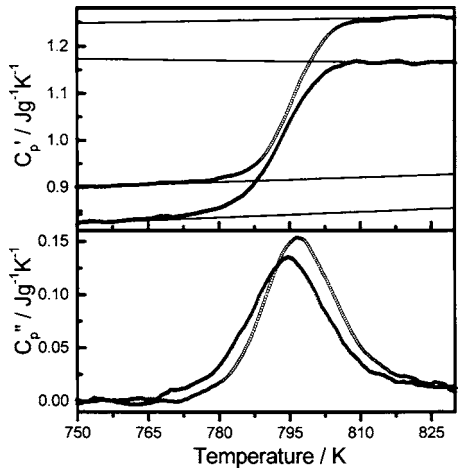

FIG. 1. Temperature dependence of real and imaginary parts of heat capacity for the KMWPO (open circles) and RbMWPO glasses (closed triangles). Extrapolated heat capacities of the glass and supercooled liquid are shown by solid lines.

Figure 1 shows the real and imaginary parts of the complex specific heat for the KMWPO and RbMWPO glasses as a function of temperature. The imaginary part of the specific heat shows a peak that corresponds to the temperature where the characteristic relaxation time of the sample $\tau(T)=1/\omega$ is the most probable. This peak gives information about glass transition T_g. The estimated glass transitions T_g are 797 K for the KMWPO glass and 795 K for the RbMWPO glass, respectively. The real part shows a sigmoid shape stepwise increase characteristic of the approach of the unrelaxed state of a glass towards its relaxed state. The magnitude of heat capacity for glass (C_p^g) and liquid (C_p^l) at the relevant temperatures was obtained by extrapolation of supercooled liquid's and glass's heat capacities, as shown by the lines drawn in Fig. 1. This approximation yielded ΔC_p, which is the contribution to the heat capacity from configurational changes involved in the α-relaxation process alone.[18] The observed heat capacity increases ΔC_p at T_g are 0.339 J g^{-1} K^{-1} (172.3 J mol^{-1} K^{-1}) for the KMWPO glass and 0.325 J g^{-1} K^{-1} (195.3 J mol^{-1} K^{-1}) for the RbMWPO glass, respectively. These values correspond to 1.37 and 1.39 C_p^l/C_p^g ratios for the KMWPO and RbMWPO glasses, respectively. A number of studies showed that such a large increase of C_p' is a characteristic feature of a fragile liquid,[17,19,20,25] indicating that the KMWPO and RbMWPO phosphates are relatively fragile liquids. Recently, a correlation between the dynamic and thermodynamic fragilities has been reexamined for a number of glass formers.[25] It has been shown that inorganic glass-forming liquids exhibit the behavior originally described by Angell[19] that the dynamic fragility index m increases as the ratio C_p^l/C_p^g increases. According to Huang and McKenna's correlation between m and C_p^l/C_p^g,[25] the fragility indices m should be about 48 and 50 for the KMWPO and RbMWPO glasses, respectively. However, it should be remembered that this correlation is not very accurate and the real values of the fragility index m, obtained

from viscosity measurements, can be significantly different from those evaluated from the heat capacity studies. Nevertheless, the estimated fragility indices suggest that the KMWPO and RbMWPO phosphates belong to the group of materials exhibiting intermediate fragility.

The relaxations of the glass formers are usually nonexponential, and comparisons are often made using the fractional exponent β in the Kolhraush-Williams-Watts function:

$$\phi(t) = \exp(-(t/\tau)^{\beta}). \quad (1)$$

It has been shown that the value of β can be estimated from the MDSC measurement.[26] In the MDSC method the shape of susceptibility $C_p^*(T)$ curves not only depends on the stretched exponent β but also on the effective value of the activation energy in the temperature domain of the loss peak. However, as was proposed by Böhmer *et al.*,[27] β can be estimated in a way that is free from an assumption about the temperature dependence of the relaxation time. In the ideal case of an exponential Debye relaxation function, the ratio of the magnitude of a loss peak (C_p'') to the dispersion step ($\Delta C_p'$) is 0.5 and this ratio becomes smaller when β decreases with increasing departures from exponential decay. This correlation has been tabulated by Moynihan *et al.* and is shown to give an accurate value of β.[28] We have estimated $C_p''/\Delta C_p'$ ratio and β was then determined using Table II from Ref. 28. The obtained values of $C_p''/\Delta C_p'(\beta)$ are 0.425 ± 0.05 (about 0.81) and 0.396 ± 0.05 (about 0.75) for the KMWPO and RbMWPO, respectively. The former studies of glass-forming materials have shown that β can also be a marker of fragility since there exists a correlation between fragility index m and β value.[25,29,30] A low value of β was shown to indicate broad relaxations in compounds which also usually exhibit high fragility. The β values obtained for the KMWPO and RbMWPO seem to be overestimated but nevertheless they are consistent with the conclusion obtained with the help of Huang and McKenna's correlation[25] that KMWPO and RbMWPO phosphates exhibit intermediate fragility. They also suggest that fragility of the RbMWPO liquid is larger than that of the KMWPO one.

Fragility of phosphate glasses is known to depend on the structure and the bond strength between the modifier and oxygen ions. It has been shown that alkali metal metaphosphates are fragile liquids with fragility index m higher than 100.[31] When alkali metal ions are replaced by Mg^{2+} ions, that exhibit stronger electric field strength (z/r^2), the fragility strongly decreases and the fragility index for the $MgO-P_2O_5$ glass is only $m=40$.[32] On the other hand, relative decrease of the P_2O_5 concentration in the glass results in fragility increase.[32,33] The KMWPO and RbMWPO glasses studied here can be regarded as obtained by adding $K_2O(Rb_2O)$ and WO_3 to $MgO-P_2O_5$ glass. The introduction of alkali metal ions would certainly increase fragility due to weak electric strength of these ions and decrease in the length of phosphate units. On the other hand, because the added W^{6+} ions have high (sixfold) coordination and may form strong covalent bonds, a decrease of fragility is expected by adding WO_3. As can be noticed, the introduction of $K_2O(Rb_2O)$ and WO_3 to $MgO-P_2O_5$ glass should have an opposite effect on the fragility and it is reasonable to expect that the studied KMWPO and RbMWPO liquids would have intermediate strength, similar as $MgO-P_2O_5$ phosphate. Similar values of the fragility indices m for the glasses studied here and the $MgO-P_2O_5$ glass are consistent with this assumption. Since the structure of the KMWPO and RbMWPO glasses is the same (see Sec. III D of the present paper), the observed increase of fragility for the Rb-containing glass can be attributed to weaker electric field strength (z/r^2) of Rb^+ when compared with K^+. This effect was previously observed for the $M_2O-Fe_2O_3-P_2O_5$ glasses (M=K,Cs), where replacement of smaller K^+ ions by much larger Cs^+ ions leads to significant increase in fragility.[34]

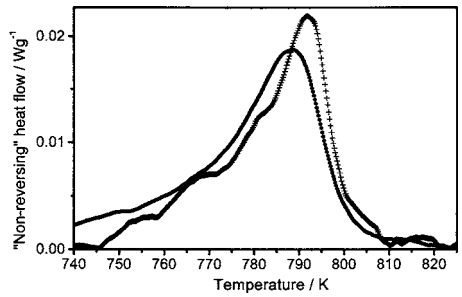

FIG. 2. Evolution of the nonreversing heat flow for the KMWPO (crosses) and RbMWPO (circles) upon heating (after subtraction the curve measured upon cooling).

The MDSC studies may also give information about the enthalpy recovery.[17] According to the free volume theory, the structural state of a glass can be characterized by the excess free volume frozen in from its supercooled liquid.[35,36] During annealing the excess free volume decreases and when the annealed sample is reheated, it absorbs energy to recover the free volume in order to attain equilibrium. This enthalpy recovery of a glass in classical DSC experiments is visible upon heating in the heat flow overshoot which culminates at the end of the heat flow jump at T_g.[17,36] This peak is the manifestation of a nonreversible phenomenon: it is not detected upon cooling. In MDSC experiment, the nonreversing component of heat flow takes into account the enthalpy recovery. In order to obtain the recovery enthalpy the curve measured upon cooling must be subtracted from those measured upon reheating.[17] Figure 2 shows the plot of nonreversing heat flow during heating after subtracting the plot upon cooling. It can be noticed that the plots for the KMWPO and RbMWPO show more or less similar magnitudes of enthalpy recovery. The estimated values of the enthalpy recovery are 15.5 and 16.2 J/g for the KMWPO and RbMWPO glasses, respectively. These values are relatively large. Such a result indicates that the obtained glasses are characterized by small concentration of defects, i.e., small free volume excess.

B. Refractive indices and elastic properties at room temperature

The unpolarized Brillouin spectra of the KMWPO and RbMWPO, presented in Fig. 3, show a strong elastic peak due to the scattering from LA modes at about 10 GHz and a second weaker peak at about 6 GHz due to light scattered from TA modes. The frequency shifts and bandwidths of the Brillouin peaks were evaluated by fitting the measured spec-

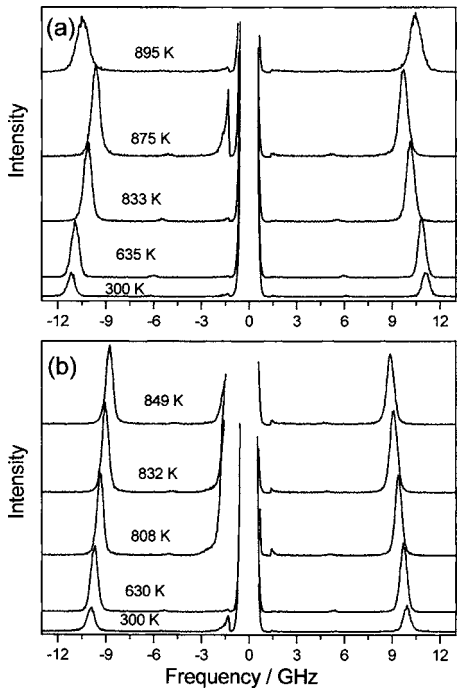

FIG. 3. Representative Brillouin spectra measured at a few temperatures for (a) the KMWPO and (b) RbMWPO glasses.

tra to the convolution of the Gaussian instrumental function with a theoretical spectral line shape (Lorenzian).

In the way proposed by Vaughan the refractive index of a material can be calculated from the formula $n=(\nu_{180}/\nu_{90})\sin 45$, where ν_{180} and ν_{90} denote Brillouin shift observed in 180° and 90° scattering geometries, respectively.[37] The obtained refractive indices are nearly the same for both glasses (1.624 and 1.618 for the KMWPO and RbMWPO glasses, respectively).

The spectra presented in Fig. 3 have been measured in symmetric 90° scattering geometry.[38] The advantage of this scattering geometry is that it allows sound velocities to be measured without knowing the refractive index of the sample.[38] Velocities were hence directly determined from the Brillouin shifts ν_B from the relation $V=\nu_{90}\lambda/2\sin 45$, where λ is the wavelength of the laser light.

In an amorphous solid, elastic strain can be described by two independent elastic constants, C_{11} and C_{44}. The Cauchy relation $2C_{44}=C_{11}-C_{12}$ allows one to determine C_{12}. From the values of longitudinal and transverse sound velocities extracted from Brillouin peaks, the constants characterizing the elastic and mechanical properties of a glass can be calculated, i.e., the longitudinal modulus $L=C_{11}=\rho V_L^2$, shear modulus $G=C_{44}=\rho V_T^2$, bulk modulus $K=L-(4/3)G$, Young's modulus $E=G(3L-4G)/(L-G)$, and Poisson's ratio $\sigma=(L-2G)/2(L-G)$, where ρ denotes density. The calculated elastic constants, using the measured densities 3.61 and 4.01 g/cm^3 for the KMWPO and RbMWPO glasses, respectively, are summarized in Table I. The calculated longitudinal, shear, bulk, and Young's moduli of the studied glasses are about 50%–40% higher than those of pure P_2O_5 glass.[39] The calculated moduli are smaller for the RbMWPO glass, indicating a decrease in hardness when K^+ ions are substituted by larger Rb^+ ions. Since the magnitude of the elastic constants of the glasses are related to the strength of the chemical bonds (provided the same topology of the arrangement of these bonds in the studied glasses is assumed), the observed changes in hardness reflect an increase in bond lengths due to more important sterical hindrance of larger Rb^+ ions compared to K^+ ions, which induces more free space between phosphate and WO_6 groups and then reduces its rigidity. Such sterical hindrance effects on elastic constants have also been observed in other glasses.[40,41]

It is worth noting that the measured spectra show also a decrease of the TA mode intensity when K^+ ions are replaced by Rb^+ ions. In isotropic systems there are only two independent photoelastic constants, P_{44} and P_{12}. Since intensity of the TA modes depends on the value of P_{44} coefficient, our results indicate its decrease in the order K > Rb. The ratio of the P_{44} and P_{12} constants can be related to the intensity I and frequency ω of the peaks in our unpolarized experiments through the relation:[42]

$$\left(\frac{P_{44}}{P_{12}}\right)^2=\frac{I(\mathrm{TA})\omega_0^2(\mathrm{TA})}{I(\mathrm{LA})\omega_0^2(\mathrm{LA})}. \tag{2}$$

The $|P_{44}/P_{12}|$ values obtained at room temperature for the KMWPO and RbMWPO are 0.061 and 0.045, respectively. The low intensity of the light scattered by TA modes is reflected in the small value of P_{44}/P_{12}. It is known that intensity of the light scattered from TA modes in Brillouin scattering is strong in liquids of highly anisotropic molecules but much lower in systems with low molecular anisotropy and where the contributions from different scattering mechanisms add out of phase.[43] Since structure of the KMWPO and RbMWPO glasses is very similar, we may assume that anisotropy of molecular units is also similar. The significant difference in intensity of TA mode can be, therefore, attributed to different contributions of scattering mechanism due to different ionic sizes of Rb^+ and K^+ as well as Rb–O and K–O bond polarizabilities. Recently a microscopic dipole-induced-dipole (DID) model was proposed for evaluating photoelastic constants in disordered isotropic solids composed of units carrying spherical polarizability.[42] The model predicts that the photoelastic constants can be determined from the relation:

TABLE I. Values of densities ρ, ratio of heat capacity change at the glass transition $\Delta C_p'$ to the heat capacity of glass C_p^g, refractive indices n, sound velocities V_L and V_T, elastic constant C_{12}, elastic moduli (L, G, K, and E), Poisson's ratio σ, and experimental ratio of the photoelastic coefficients P_{44} and P_{12}.

Composition	ρ (g/cm^3)	$\Delta C_p'/C_p^g$	n	V_L (m/s)	V_τ (m/s)	C_{12} (GPa)	L (GPa)	G (GPa)	K (GPa)	E (GPa)	σ	P_{44}/P_{12}
KMWPO	3.61	1.370	1.624	4189	2323	24.4	63.4	19.5	37.4	49.9	0.278	0.061
RbMWPO	4.01	1.385	1.618	3735	2061	21.9	56.0	17.0	33.2	43.7	0.281	0.045

$$\left[\frac{P_{44}}{P_{12}}\right]_{\mathrm{DID}} = \frac{0.2(\varepsilon-1)}{1+0.2(\varepsilon-1)}, \tag{3}$$

where $\varepsilon = n^2$ is the dielectric constant at the laser frequency. Our evaluations of Eq. (3) give the values 0.247 and 0.244 for the KMWPO and RbMWPO, respectively. As can be noticed a deviation between the prediction of the DID model and the measured values of the photoelastic ratio is large. This result clearly indicates that some other scattering mechanisms are also important in these phosphates. It has been emphasized in Ref. 42 that the TA intensity can be well predicted with the simplified DID for van der Waals glasses. However, the presence of strong covalent bonds gives rise to different polarizability induction terms.[42] The most usual term represents the contribution of soft binding electrons to the molecular polarizability.[42] These bond polarizability effects are "local" contributions, which are very difficult to estimate. It seems, therefore, that large difference between the experimental and theoretical values of P_{44}/P_{12} for the studied glasses can be attributed to large contributions of bond polarizability effects that add out of phase. It is also worth noting that the difference between theoretical and experimental values of the photoelastic ratio is significantly smaller than that observed for silicate glasses (0.4).[42] The better agreement of Eq. (3) with the values of P_{44}/P_{12} measured in our glasses, with respect to those measured in silicate glasses, can be most likely explained by presence of weaker covalent bonds in phosphates when compared to silicates.

Poisson's ratios for the studied glasses are in the range of 0.27–0.28. Previous studies on the relation of Poisson's ratio with the glass structure showed that σ was greater than 0.25 when the ions themselves are deformed under stress in addition to the network distortion.[44–46] Moreover, the L/G (or G/C_{12}) ratio is an indicator of the character of the force field: if atoms interact through a central potential, $G/C_{12}=1$ ($L/G=3$), if through noncentral potential, $G/C_{12}<1$ ($L/G>3$).[39,47] The G/C_{12} values for our glasses are around 0.8, indicating noncentral forces. These values are between that of pure P_2O_5 glass (0.7) and Fe_2O_3–P_2O_5 glass (values close to 1).[39]

C. Temperature dependence of elastic moduli

The temperature dependence of sound velocities, and Poisson's and G/C_{12} ratios is shown in Fig. 4. The rigidity markedly decreases with increasing temperature, as evidenced through decrease of longitudinal sound velocity with increasing temperature. The rate of decrease is significantly higher above T_g. Such a behavior is generally observed in glass transitions and can be attributed to the fact that the temperature dependence of viscosity in a supercooled liquid state is higher than in a glassy state. Thus, the glass transition temperature T_g can be determined from the change of slope of the temperature-dependent sound velocity. The obtained hence T_g temperatures are in good agreement with those obtained from heat capacity studies. As can be noticed the temperature behavior of longitudinal and transverse sound velocities (and the corresponding longitudinal and shear moduli, not shown in Fig. 4) is linear both below and above

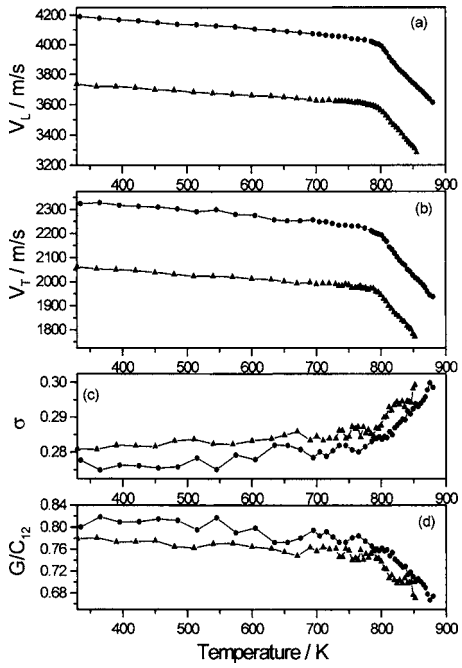

FIG. 4. Temperature dependences of (a) longitudinal sound velocity, (b) transverse sound velocity, (c) Poisson's ratio σ, and (d) a ratio of shear modulus G to C_{12} elastic constant for KMWPO (circles) and RbMWPO (triangles). Lines are guides for the eyes.

T_g. The linear fit of L and G moduli below T_g yields $L=66.95-0.0104T$ ($L=58.64-0.0082T$) and $G=20.99-0.0039T$ ($G=18.09-0.0031T$) for the KMWPO (RbMWPO). The corresponding values above T_g are $L=159.46-0.128T$ ($L=158.01-0.134T$) and $G=50.79-0.048T$ ($G=52.70-0.047T$) for the KMWPO (RbMWPO.). These data show that the slopes of the corresponding elastic moduli versus temperature are very similar for the KMWPO and RbMWPO above T_g, indicating that the network of the both phosphates degrades in a similar rate upon heating. It is interesting to notice that Poisson's ratios for the studied glasses increase significantly above T_g whereas the G/C_{12} values decrease above T_g. This result can be attributed to a significant increase of deformation of the structural units upon heating.

As mentioned above the KMWPO and RbMWPO are far from showing central potential and Cauchy relation, $L/G=3$, does not apply in its original form. However, it has been found that a Cauchy-type relation holds across the glass transition of different liquids:

$$L_\infty = A + BG_\infty, \tag{4}$$

where A is a system-dependent constant and B is found always close to 3.[11,48,49] In order to verify the validity of Cauchy-type relation in our glasses the behavior of L and G is compared with Eq. (4). Figure 5 shows that a linear relation is fulfilled within experimental uncertainty, giving $A=11.03\pm0.29$ GPa (9.72 ± 0.33 GPa) and $B=2.67\pm0.017$ (2.71 ± 0.022) as best-fit parameters for the KMWPO (RbMWPO). The linear relationship is simultaneously valid for the glassy and the liquid state with the same A and B parameters. The parameter B is lower than 3 but this departure from the expected $B=3$ value may be attributed, as emphasized by

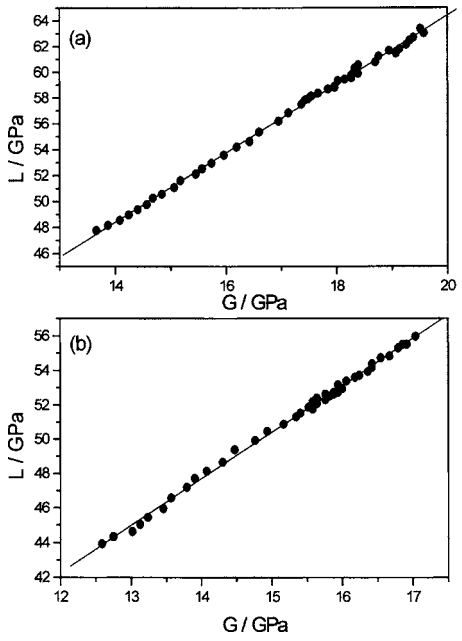

FIG. 5. Linear fit of the longitudinal elastic modulus vs the transverse elastic modulus of (a) KMWPO and (b) RbMWPO.

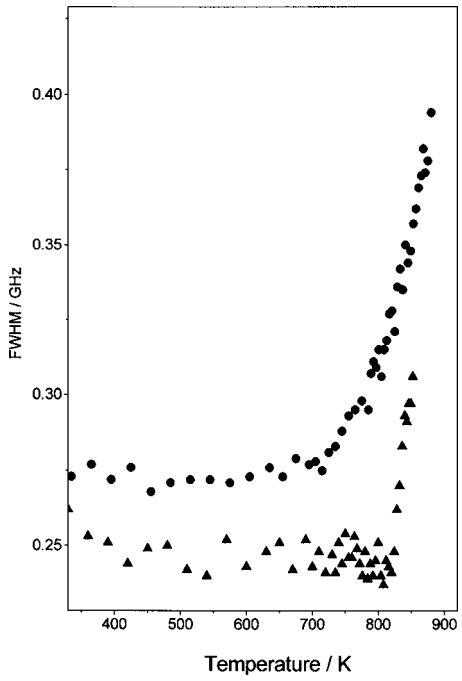

FIG. 6. Temperature dependence of full width at half maximum of the LA modes for KMWPO (circles) and RbMWPO (triangles).

Krüger *et al.*,[49] to some errors due to weak intensity of transverse mode, the onset of relaxations at higher temperature, etc. Krüger *et al.* had shown that the following relationship yields the parameters A and B:[49]

$$A = \frac{2C_{11}(T_g)(\gamma_4^{l,g} - \gamma_1^{l,g})}{1 + 2\gamma_4^{l,g}}, \tag{5}$$

$$B = \frac{C_{11}(T_g)}{C_{44}(T_g)} - \frac{2C_{11}(T_g)(\gamma_4^{l,g} - \gamma_1^{l,g})}{(1 + 2\gamma_4^{l,g})C_{44}(T_g)}, \tag{6}$$

where $\gamma_1^{l,g}$ and $\gamma_4^{l,g}$ denote longitudinal and transverse mode Grüneisen parameters, respectively (superscripts l and g correspond to liquid and glassy states, respectively). The mode Grüneisen parameters can be calculated from the formula:[50]

$$\gamma_i = \frac{\rho(T_g)[d\omega_i(T)/dT]}{\omega(T_g)[d\rho(T)/dT]}, \tag{7}$$

where $i=1$ and 4 corresponds to the longitudinal and transverse acoustic modes, respectively, ω (T) denotes frequency of the acoustic mode, and $\rho(T)$ is density. Since we do not know the temperature dependence of density, we cannot calculate directly the mode Grüneisen parameters from Eq. (7). We may, however, calculate with the help of Eq. (7) and the experimental data the ratios $\gamma_4^{l,g}/\gamma_1^{l,g}$, and then use the obtained values to calculate the mode Grüneisen parameters from Eq. (6). The estimated values are $\gamma_4^g=0.36$, $\gamma_1^g=0.28$, $\gamma_4^l=0.38$, and $\gamma_1^l=0.30$ for KMWPO and $\gamma_4^g=0.66$, $\gamma_1^g=0.55$, $\gamma_4^l=0.81$, and $\gamma_1^l=0.68$ for RbMWPO. The obtained values are an order of magnitude smaller than those found for poly-trimethyl-hexamethylen-terephtalamid,[49] indicating that the studied glasses are characterized by relatively weak elastic anharmonicity. One can also notice that the anharmonicity of the RbMWPO phosphate is larger than anharmonicity of the KMWPO. This result also supports our conclusion derived from the heat capacity studies that RbMWPO is more fragile than KMWPO since it has been shown previously that there is a correlation between the Grüneisen parameters and fragility, i.e., the higher are the Grüneisen parameters the more fragile is the liquid.[5]

The obtained data show also that the bandwidth of the LA modes starts to rise significantly above T_g due to decrease of the structural relaxation time (see Fig. 6). However, the bandwidth increase is relatively small and the observed Brillouin peaks are nearly symmetric, indicating that the relaxation times are still relatively long. This behavior confirms our conclusion that the studied KMWPO and RbMWPO phosphates are stronger than typical molecular glass formers.

D. Raman scattering in the 100–1300 cm^{-1}: Glass structure

Raman spectra of the KMWPO and RbMWPO glasses in the 100–1300 cm^{-1} region are shown in Fig. 7. The spectra are dominated by very intense and strongly polarized band near 935 cm^{-1}. The comparison of the measured spectra with the previous results obtained for crystalline $Rb_2MgWO_2(PO_4)_2$ and $(80-0.8x)NaPO_3-(20-0.2x)BaF_2-xWO_3$ glass allows us to assign this band to symmetric stretching mode of the WO_6 octahedra.[51,52] The Raman spectra exhibit also two bands near 885 and 820 cm^{-1}. The former depolarized band can be assigned to the asymmetric stretching vibration of the WO_6 octahedra. The second band could be assigned to stretching vibrations of the W–O–W bridging modes, as suggested in the studies of fluorophosphate glasses.[52] However, this band was observed only for high concentration of WO_3 oxide (more than 30%) in the glass matrix.[52] In our case it is not plausible to suppose that this band originates from the W–O–W bonds since the concentration of WO_3 oxide is relatively low.

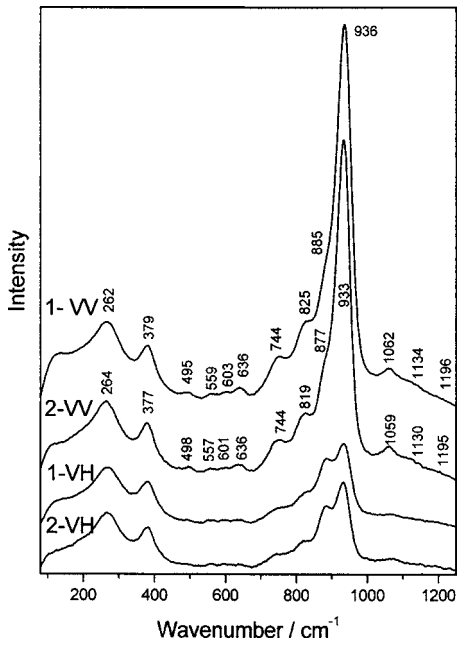

FIG. 7. Raman spectra of the KMWPO (1) and RbMWPO (2) glasses in VV and VH polarizations.

Moreover, our study of the crystalline $Rb_2MgWO_2(PO_4)_2$ also showed the presence of a similar band at slightly higher frequency, 839 cm^{-1}, although the crystal structure does not contain any W–O–W bridging bonds.[51] We assign, therefore, the 820 cm^{-1} band to the stretching vibration of the W–O–P bridges, in agreement with the assignment proposed for $Na_2O-WO_3-P_2O_5$ glasses.[33] The presence of WO_6 octahedra gives also rise to two intense unpolarized bands near 265 and 380 cm^{-1} that can be assigned to the bending vibrations.[52]

Apart from the discussed above bands, the Raman spectra show the presence of two very characteristic bands near 1060 and 744 cm^{-1}. These bands can be assigned to symmetric stretch of the terminal $-PO_3$ group and the P–O–P symmetric stretching mode of pyrophosphate units (Q^1 tetrahedra),[33,52–54] indicating that the phosphate polyhedra are present in the glass structure mainly in the form of pyrophosphate groups. It is worth noting, however, that the studied glasses contain also small concentration of metaphosphate groups (Q^2 tetrahedra) because the measured Raman spectra exhibit bands near 1200 and 1130 cm^{-1} that can be assigned to asymmetric and symmetric stretches of the PO_2 group, respectively.[52–54] These metaphosphate groups are most likely present in the form of the $(P_3O_9)^{3-}$ rings since the Raman spectra exhibit a band near 638 cm^{-1} that is characteristic of the bending mode of the $(P_3O_9)^{3-}$ anion.[55] The Raman spectra exhibit also a few weak bands in the region of 490–600 cm^{-1} that originate from bending vibrations of the phosphate polyhedra. A question arises whether the studied glasses contain also orthophosphate groups. It is well known that the most intense Raman band of the orthophosphate groups should be present near 950–980 cm^{-1}.[53,54] Unfortunately, the WO_6 groups present in the studied glasses exhibit very intense band near 935 cm^{-1} and, therefore, a much weaker band characteristic for the orthophosphate groups may not be resolved. We conclude, therefore, that although the Raman data do not give any evidence that the orthophosphate groups are present in the glass structure, the presence of small concentration of these groups in the glass cannot be excluded.

Although the studied glasses have very similar structures, composed mainly of pyrophosphate groups separated by WO_6, magnesium-oxygen, and alkali metal-oxygen polyhedra, closer inspection shows that bandwidth of many observed Raman bands decreases when smaller K^+ cations are replaced by larger Rb^+ cations. The difference in the bandwidth can be attributed to fluctuations of the metaphosphate group conformations, ion coordination numbers, etc. The wider Raman bands for the KMWPO glass implies, therefore, a richer variety of environments into which the phosphate and WO_6 structural units can be found in this material. It is worth to note that very similar behavior was observed previously for $LiPO_3$ and $RbPO_3$ metaphosphates.[56] The increase of some Raman bandwidths for $LiPO_3$ was explained by the fact that Li^+ ions are much smaller than Rb^+ ones and have the possibility to occupy more sites in the structure.[56] The same arguments can probably be used to explain increase of bandwidth when larger Rb^+ ions are replaced by smaller K^+ ions.

It is also noticed that the Raman bands, observed above 1000 cm^{-1}, shift towards lower frequency when K^+ ions are replaced by Rb^+ cations. The former studies of phosphates showed that vibrations of the PO_2 and $-PO_3$ terminal groups can be regarded as localized and that the energy of particular vibration is determined by its immediate surrounding.[56–58] The wave number of these bands was shown to decrease with decreasing field strength of the modifying ions, which is proportional to z/r^2, where z is the ion charge and r is the ionic radius.[56,58] The observed shifts towards lower frequency when K^+ is replaced by Rb^+ can be, therefore, explained by weaker field strength of the Rb^+ cations.

E. Low-frequency Raman scattering: Boson peak

It is well known that a characteristic feature of a glass is appearance of so-called Boson peak corresponding to an excess of low-frequency vibrational states in respect to the predictions of the Debye theory that can be observed in the Raman spectra below 120 cm^{-1}.[13–16] Figure 8 presents the reduced low-frequency Raman spectra of KMWPO and RbMWPO glasses in two different reduction schemes:

$$I^{\mathrm{red}}(\omega) = \frac{I^{\mathrm{exp}}(\omega)}{\omega[n(\omega,T)+1]} \propto \frac{g(\omega)C(\omega)}{\omega^2}, \tag{8}$$

$$\chi''(\omega) = \frac{I^{\mathrm{exp}}(\omega)}{[n(\omega,T)+1]} \propto \frac{g(\omega)C(\omega)}{\omega}, \tag{9}$$

where $I^{\mathrm{exp}}(\omega)$, $C(\omega)$, $g(\omega)$, and $n(\omega,T)$ denote the experimentally measured scattered Raman intensity, the photon-phonon or Raman coupling coefficient, vibrational density of states, and the Bose-Einstein occupation number, respectively. It is worth noting that above 120 cm^{-1} Raman intensity increases due to contribution from the vibrational mode centered near 262–264 cm^{-1}. Since this contribution influ-

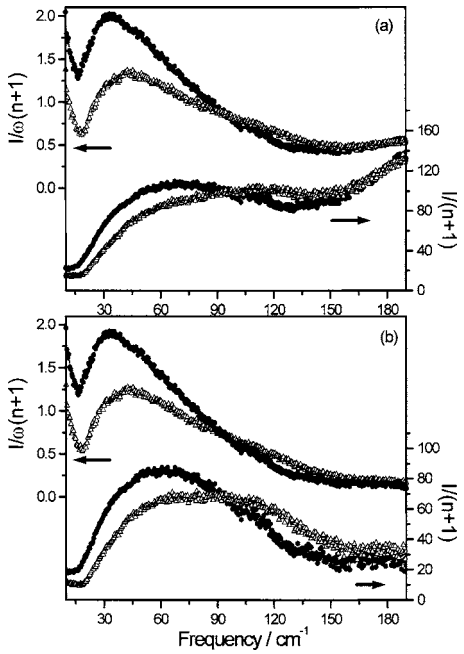

FIG. 8. (a) Low-frequency VH Raman data in two reduction schemes for the KMWPO (triangles) and RbMWPO (circles). (b) Same as (a) but after subtraction of the contribution coming from the vibrational mode near 262–264 cm^{-1}. This contribution was estimated by deconvolution of the Raman spectra in the 180–500 cm^{-1} range into two Lorenzians centered near 264–264 and 379–377 cm^{-1}.

ences the shape of the higher frequency part of the Boson peak, we present also the data after subtraction this contribution from the measured spectra (see lower panel of Fig. 8). The $I^{red}(\omega)$ plots show the presence of a very broad asymmetric Boson peak. The maximum frequency of the Boson peak shifts from 43 cm^{-1} for the KMWPO glass to 35 cm^{-1} for the RbMWPO glass. The former studies of alkali metaphosphates and alkali silicate glasses also showed that frequency of the Boson peak decreases with increasing mass of the alkali metal.[59,60] This dependence was approximately inversely proportional to the square root of the atomic mass for alkali silicate glasses or inversely proportional to the square of alkali metal-oxygen bond distances for alkali metaphosphates.[59,60] In our case this dependence is similar as that observed for the metaphosphates. The $\chi''(\omega)$ plots show also very clearly that the maximum of the Boson peak shifts to higher frequency and its bandwidth increases significantly when Rb^+ is replaced by K^+.

Changes of the Boson peak intensity and frequency were very often related to changes in some glass properties. For instance, it has been claimed that frequency of the Boson peak can be related to the length scale at which the molecular structure becomes important.[61,62] Recently, the validity of empirical correlations between a spectral characteristic of the Boson peak and a specific property of the glass has been questioned since it has been shown that the maximum frequency of the Boson peak is not directly related to the maximum distribution of the excess of states.[16] On the contrary, it is sensitive to the type of the tails of the low-frequency edge of such a distribution. It has been shown that the change of the excess distribution tails from convex (semicircular type) to concave (Gaussian) will result in reducing of the Boson peak asymmetry and shifting the frequency of its maximum to higher energies.[16] Another problem is that the spectral characteristic of the Boson peak is influenced by the contribution of the Debye density of states $[g^D(\omega)]$.[16] Having these facts in mind, it is clear that the true excess vibrational density of states, i.e., $g(\omega)^{exc}=g(\omega)-g^D(\omega)$, should be analyzed in order to obtain some information about glass properties. The $g^D(\omega)$ can be easily calculated from the formula $g^D(\omega)=3\omega^2/\omega_D^3$, where the Debye frequency can be estimated from the Brillouin data (the estimated ω_D are 219.0 and 190.3 cm^{-1} for the KMWPO and RbMWPO glasses, respectively). Unfortunately, in order to estimate the absolute value of $g(\omega)$ from Raman scattering a proper normalization factor is needed which can be derived from the low-temperature heat capacity studies.[63] Since such data are not available for the studied glasses, we cannot estimate the $g(\omega)^{exc}$ from our Raman measurements. However, the former studies showed that $C(\omega)$ is proportional to ω in many glasses up to frequency at which the Boson peak exhibits maximum intensity,[64] or even up to half of the Debye frequency.[63] If we assume that $C(\omega)\propto\omega$, the $\chi''(\omega)$ plots in Fig. 8 would be proportional to $g(\omega)$, at least in the lower frequency range. Having in mind that $g^D(\omega)\propto\omega^2$, it is clear from the shape of these plots that the frequency distribution of $g(\omega)^{exc}$ corresponds approximately to convexlike tails. This form is consistent with recent predictions of the Euclidean random matrix theory,[65,66] as already noticed by Yannopoulos *et al.*[16]

The change in the maximum frequency of the Boson peak when Rb^+ are replaced by K^+ ions in the studied glasses can be attributed to at least two contributions. Firstly, the $g(\omega)^{exc}$ may shift towards higher frequency in the KMWPO glass due to "strengthening" of the involved vibrational modes. This explanation is very likely since the KMWPO glass has smaller molar volume (140.8 cm^3/mol, in comparison with 149.9 cm^3/mol for the RbMWPO) and the K^+ ions have stronger field strength. Secondly, the substitution of K^+ for Rb^+ may also influence the distribution of $g(\omega)^{exc}$. However, the present results do not allow us to estimate this contribution.

IV. CONCLUSIONS

The performed Raman studies showed that the main structural units of the network are pyrophosphate groups. These glasses contain, however, also some smaller amount of metaphosphate and orthophosphate units. Raman study revealed also that substitution of K^+ for Rb^+ ions leads to a richer variety of environments into which the phosphate and WO_6 structural units can be found. This behavior was explained by the fact that K^+ ions are much smaller than Rb^+ ones and have the possibility to occupy more sites in the structure.

Heat capacity and Brillouin studies showed that substitution of K^+ ions for Rb^+ ions leads to decrease of fragility and anharmonicity as well as increase of the elastic moduli and the maximum frequency of the Boson peak. These effects were shown to be related, at least partially, to decrease of the Rb–O bond strength with respect to the K–O bond strength. Our results showed also that a linear relation be-

tween shear and longitudinal moduli of the studied phosphates holds across the glass transition with an angular coefficient close to 3. These results confirmed that the Cauchy-type relation is valid for many glass-forming materials, as reported recently.[11,48,49] We showed also that the correlation between the angular coefficient in the Cauchy-type relation, elastic moduli, and Grüneisen parameters can be used as a suitable tool for estimation of elastic anharmonicity, even if the temperature dependence of density is not known.

Low-frequency Raman scattering studies revealed that the maximum frequency of the observed Boson peaks shifts from 43 cm^{-1} for the KMWPO glass to 35 cm^{-1} for the RbMWPO glass. The analysis of the Boson peak shape confirmed that it can be explained assuming approximately the convexlike frequency distribution of the excess density of states. The change in the maximum frequency of the Boson peak when Rb^+ are replaced by K^+ ions in the studied glasses can be attributed to "strengthening" of the involved vibrational modes and possibly also to some change in the distribution of the excess density of states.

[1] C. A. Angell, K. L. Ngai, G. B. McKenna, P. F. McMillan, and S. W. Martin, J. Appl. Phys. **88**, 3113 (2000).
[2] N. J. Tao, G. Li, and H. Z. Cummins, Phys. Rev. B **45**, 686 (1992).
[3] C. Dreyfus, A. Aouadi, J. Gapinski, M. Matos-Lopes, W. Steffen, A. Patkowski, and R. M. Pick, Phys. Rev. E **68**, 11204 (2003).
[4] J. Wiedersich, S. A. Adichtchev, and E. Rössler, Phys. Rev. Lett. **84**, 2718 (2000).
[5] S. Kojima, V. N. Novikov, and M. Kodama, J. Chem. Phys. **113**, 6344 (2000).
[6] H. P. Zhang, A. Brodin, H. C. Barshilia, G. Q. Shen, and H. Z. Cummins, Phys. Rev. E **70**, 11502 (2004).
[7] C. Dreyfus, A. Aouadi, R. M. Pick, T. Berger, A. Patkowski, and W. Steffen, Eur. Phys. J. B **9**, 401 (1999).
[8] V. Bogdanov, A. Kisliuk, S. Mamedov, S. Nemilov, D. Quitmann, and M. Soltwisch, J. Chem. Phys. **119**, 4372 (2003).
[9] W. Götze and L. Sjögren, Rep. Prog. Phys. **55**, 241 (1992).
[10] S. N. Yannopoulos, G. N. Papatheodorou, and G. Fytas, Phys. Rev. B **60**, 15131 (1999).
[11] F. Scarponi, L. Comez, D. Fioretto, and L. Palmieri, Phys. Rev. B **70**, 54203 (2004).
[12] R. K. Brow, J. Non-Cryst. Solids **263–264**, 1 (2000).
[13] W. Schirmacher, G. Diezemann, and C. Ganter, Phys. Rev. Lett. **81**, 136 (1998).
[14] S. N. Taraskin, Y. L. Loh, G. Natarajan, and S. R. Elliot, Phys. Rev. Lett. **86**, 1255 (2001).
[15] A. I. Chumakov, I. Sergueev, U. Van Bürck, W. Schirmacher, T. Asthalter, R. Rüffer, O. Leupold, and W. Petry, Phys. Rev. Lett. **92**, 245508 (2004).
[16] S. N. Yannopoulos, K. S. Andrikopoulos, and G. Ruocco, J. Non-Cryst. Solids **352**, 4541 (2006).
[17] O. Bustin and M. Descamps, J. Chem. Phys. **110**, 10982 (1999).
[18] E. Tombari, S. Presto, G. Salvetti, and G. P. Johari, J. Chem. Phys. **117**, 8436 (2002).
[19] C. A. Angell, in *Relaxations in Complex Systems*, edited by K. Ngai and G. B. Wroght (Naval Research Laboratory, Washington D.C., 1985).
[20] K. Ito, C. T. Moynihan, and C. A. Angell, Nature (London) **398**, 492 (1999).
[21] Y. Matsuda, C. Mtsui, Y. Ike, M. Kodama, and S. Kojima, J. Therm Anal. Calorim. **85**, 725 (2006).
[22] U. Peuchert, L. Bohaty, and J. Schreuer, Acta Crystallogr., Sect. C: Cryst. Struct. Commun. **53**, 11 (1997).
[23] R. Haase, *Thermodynamics of Irreversible Processes* (Dover, New York, 1990).
[24] S. R. Aubuchon and P. S. Gill, J. Therm. Anal. **49**, 1039 (1997).
[25] D. Huang and G. B. McKenna, J. Chem. Phys. **114**, 5621 (2001).
[26] L. Carpentier, O. Bustin, and M. Descamps, J. Phys. D **35**, 402 (2002).
[27] R. Böhmer, E. Sanchez, and C. A. Angell, J. Phys. Chem. **96**, 9089 (1992).
[28] C. T. Moynihan, L. P. Boesch, and N. L. Laberge, Phys. Chem. Glasses **14**, 122 (1973).
[29] R. Böhmer, K. L. Ngai, C. A. Angell, and D. J. Plazek, J. Chem. Phys. **99**, 4201 (1993).
[30] K. L. Ngai and R. W. Rendell, Phys. Rev. B **41**, 754 (1990).
[31] D. L. Sidebottom, P. F. Green, and R. K. Brow, J. Mol. Struct. **479**, 219 (1999).
[32] R. Sato, T. Komatsu, and K. Matusita, J. Non-Cryst. Solids **201**, 222 (1996).
[33] S. Muthupari and K. J. Rao, J. Phys. Chem. Solids **57**, 553 (1996).
[34] X. Fang, C. S. Ray, and D. E. Day, J. Non-Cryst. Solids **319**, 314 (2003).
[35] M. H. Cohen and G. S. Grest, Phys. Rev. B **20**, 1077 (1979).
[36] P. Wen, M. B. Tang, M. X. Pan, D. Q. Zhao, Z. Zhang, and W. H. Wang, Phys. Rev. B **67**, 212201 (2003).
[37] J. M. Vaughan, *Fabry-Perot Interferometer: History, Theory, Practice, and Applications* (A. Hilger, Bristol, 1989).
[38] C. H. Whitfield, E. M. Brody, and W. A. Bassett, Rev. Sci. Instrum. **47**, 942 (1976).
[39] K. H. Chang, T. H. Lee, and L. G. Hwa, Chin. J. Phys. (Taipei) **41**, 414 (2003).
[40] J. C. Sabadel, P. Armand, F. Terki, J. Pelous, D. Cachau-Herreillat, and E. Philippot, J. Phys. Chem. Solids **61**, 1745 (2000).
[41] D. J. M. Burkhard, Solid State Commun. **101**, 903 (1997).
[42] P. Benassi, V. Mazzacurati, G. Ruocco, and G. Signorelli, Phys. Rev. B **48**, 5987 (1993).
[43] A. Patkowski, W. Steffen, H. Nilgens, and E. W. Fischer, J. Chem. Phys. **106**, 8401 (1997).
[44] T. Smyth, J. Am. Ceram. Soc. **42**, 277 (1959).
[45] B. Bridge, N. D. Patel, and D. N. Waters, Phys. Status Solidi A **77**, 655 (1983).
[46] C. C. Chen, Y. J. Wu, and L. G. Hwa, Mater. Chem. Phys. **65**, 306 (2000).
[47] M. Born and K. Huang, *Dynamical Theory of Crystal Lattices* (Oxford University Press, Oxford, 1966).
[48] H. Yamura, M. Matsukawa, T. Otani, and N. Ohtori, Jpn. J. Appl. Phys., Part 1 **38**, 3175 (1999).
[49] J. K. Krüger, J. Baller, T. Britz, A. le Countre, R. Peter, R. Bactavatchalou, and J. Schreiber, Phys. Rev. B **66**, 12206 (2002).
[50] E. M. Brody, C. J. Lubell, and C. L. Beatty, J. Polym. Sci., Polym. Phys. Ed. **13**, 295 (1975).
[51] M. Maczka, A. Waskowska, and J. Hanuza, J. Solid State Chem. **179**, 103 (2006).
[52] G. Poirier, Y. Messaddeq, S. J. L. Ribeiro, and M. Poulain, J. Solid State Chem. **178**, 1533 (2005).
[53] M. A. Karakassides, A. Saranti, and I. Koutselas, J. Non-Cryst. Solids **347**, 69 (2004).
[54] J. Schwartz, H. Ticha, L. Tichy, and R. Mertens, J. Optoelectron. Adv. Mater. **6**, 737 (2004).
[55] A. M. Efimov, J. Non-Cryst. Solids **209**, 209 (1997).
[56] J. Swenson, A. Matic, A. Brodin, L. Börjesson, and W. S. Howells, Phys. Rev. B **58**, 11331 (1998).
[57] K. B. Richard, J. Non-Cryst. Solids **263&264**, 1 (2000).
[58] G. B. Rouse, P. J. Miller, and W. M. Risen, J. Non-Cryst. Solids **28**, 193 (1978).
[59] P. L. Miller, J. Chem. Phys. **71**, 997 (1979).
[60] C. McIntosh, J. Toulouse, and P. Tick, J. Non-Cryst. Solids **222**, 335 (1997).
[61] S. R. Elliot, in *Physics of Amorphous Materials* (Longman Scientific & Technical, Essex, 1990), p. 139.
[62] C. Levelut, N. Gaimes, F. Terki, G. Cohen-Solal, J. Pelous, and R. Vacher, Phys. Rev. B **51**, 8606 (1995).
[63] A. P. Sokolov, A. Kisliuk, and D. Quitmann, Phys. Rev. B **48**, 7692 (1993).
[64] A. Fontana, R. Dell'Anna, M. Montagna, F. Rossi, G. Viliani, G. Ruocco, M. Sampoli, U. Buchenau, and A. Wischnewski, Europhys. Lett. **47**, 56 (1999).
[65] G. Parisi, J. Phys.: Condens. Matter **15**, S765 (2003).
[66] T. S. Grigera, V. Martin-Mayor, G. Parisi, and P. Verrocchio, Nature (London) **422**, 289 (2003).